DOI: 10.26599/FSHW.2026.9251037

Contents lists available at SciOpen

Food Science and Human Wellness

journal homepage: https://www.sciopen.com/journal/2097-0765

China Food Publishing Co.

Lewis Bases-Assisted Enhanced SERS for Ultra-Sensitive Detection of Pesticide Residues

Jun Cheng[a,b,1], Songting Chen[a,b,1], Yi Wang [a,b], Nuohang Wan[a,b], Songlei wang[c], Junni Zhao[d], Wei Ji[e]* and Yunfei Xie[a,b]*

[a] *School of Food Science and Technology, Jiangnan University, No.1800 Lihu Avenue, Wuxi 214122, Jiangsu Province, China*

[b] *Key Laboratory of Screening, Prevention, and Control of Food Safety Risks, State Administration for Market Regulation, Wuxi 214122, Jiangsu Province, China*

[c] *College of Food Science and Engineering, Ningxia University, Yinchuan 750021, Ningxia Hui Autonomous Region, China*

[d] *Mengniu Dairy (Ningxia) Co., Ltd., Yinchuan City 750403, Ningxia Hui Autonomous Region, China*

[e] *College of Chemistry, Chemical Engineering and Resource Utilization Northeast Forestry University, Harbin 145040, China*

ABSTRACT: The ability to detect pesticide residues at trace levels is crucial for ensuring consumer health and complying with regulatory standards. Herein, we constructed a hydrophobic layer SERS substrate of silver nanoparticles on the glass surface, utilizing Lewis bases to enhance the interaction between the pesticide and the substrate. This facile method enables the ultrasensitive detection of 6-benzylaminopurine (6-BA), with the lowest detection limit decreasing from 0.01 mg/L to 5×10^{-5} mg/L. More importantly, the detection limit of 6-BA in bean sprouts reached 5×10^{-4} mg/kg, which is 20 times lower than the allowable residue level (0.01 mg/kg) in legumes set by the EU. Furthermore, the SERS signals of several pesticides, including kinetin, carbendazim, and imidacloprid, can also be enhanced by an order of magnitude. We believe that this method expands the applicability of SERS technology for practical pesticide residue detection, offering a simpler and more sensitive means for analyzing various pesticide contaminants.

Keywords: SERS; Lewis Bases; Ultrasensitive; Testing methods; 6-Benzylaminopurine (6-BA)

1. Introduction

Given the potential health risks associated with pesticide residues in food, this issue has garnered increasing attention[1, 2]. The ability to detect these residues at trace levels is crucial for ensuring consumer health and compliance with regulatory standards[3]. Among these substances, 6-benzylaminopurine (6-BA), a widely utilized plant growth regulator, has attracted considerable attention due to its extensive application in agricultural production[4]. Nevertheless, irregular usage or excessive residues of 6-BA may pose significant risks to human health, including potential endocrine disruption and toxic effects. Current methods for detecting pesticides include gas chromatography[5], liquid chromatography[6], and enzyme-linked

[1] These authors contributed equally to this work: Jun Cheng; Shunqian Zhuang
***Corresponding author.**
jiwei@nefu.edu.cn; xieyunfei@jiangnan.edu.cn

Received 6 August 2025
Received in revised from 7 September 2025
Accepted 18 November 2025

immunosorbent assays (ELISA)[7]. However, both gas and liquid chromatography have significant drawbacks, including high equipment costs and lengthy analysis times. These limitations can hinder their practicality for routine pesticide monitoring.

Nevertheless, surface-enhanced Raman scattering (SERS) spectroscopy exhibits considerable potential for application owing to its high sensitivity and rapid detection capabilities[8]. It can effectively overcome the limitations of other methods in the detection of 6-BA. SERS technology can provide detailed molecular information without the need for complex sample preparation. Among its various applications, SERS spectroscopy has emerged as an effective, straightforward, and highly sensitive method for detecting trace analytes[9-11]. SERS significantly amplifies Raman signals through interactions between molecules and metallic nanostructures, primarily via two mechanisms: electromagnetic enhancement[12] and chemical enhancement[13]. Electromagnetic enhancement occurs when analytes are adsorbed onto rough metal surfaces, resulting in localized electromagnetic field amplification[14], while chemical enhancement involves charge transfer interactions between the analyte and the metal, further boosting the signal[15-17].

Building on the principles of SERS detection, this technology has found extensive applications in food safety research, particularly in the detection of pesticide and veterinary drug residues[18-21]. However, due to the limited applicability of different SERS substrates in the detection of pesticide residues, there are also defects such as unstable detection results and interference from complex food matrices. These challenges arise primarily from the varying characteristics of pesticides and the differing enhancement effects of SERS substrates on the Raman signals of different pesticides. As a result, the effective use of SERS in this context frequently necessitates complex design and fine-tuning of the SERS substrates[22]. This complexity limits the simplicity and universality of SERS technology in practical applications[23]. Therefore, there is an urgent need for a more universal approach that employs simpler and more cost-effective SERS substrates for detecting various pesticide residues. To address this challenge, we developed a universal strategy based on the synergistic integration of a physically functionalized substrate with a tunable chemical enhancement process, thereby circumventing the need for complex substrate engineering. Reports indicate that the hydrophobic substrate effectively pre-concentrates target molecules at the SERS "hot spots"[24, 25], while the subsequent introduction of OH^- or H^+, tailored to the specific charge characteristics of the analyte, optimizes their chemical state and charge[26-28]. This dual approach maximizes the chemical enhancement effect, leading to a substantial improvement in detection sensitivity.

Herein, we synthesized a positively charged silver nanoparticle SERS substrate with hydrophobic enrichment properties on a glass surface. This hydrophobic material aids in concentrating analytes from liquid samples, thereby increasing their concentration and detectability in specific environments. Meanwhile, we introduced OH^- into the detection system based on Lewis acid-base theory to modify the hydrolysis equilibrium of the target pesticides. The positive charge generated by the hydrolysis of the 6-BA pesticide significantly enhanced the detection efficacy. Notably, the detection limit of the 6-BA standard solution has been decreased from 0.01 mg/L to 5×10^{-5} mg/L, and the detection limit in the actual bean sprout system is

5×10^{-4} mg/kg. This SERS detection method, which synergistically combines hydrophobic enrichment and charge alteration for chemical enhancement, can be applied to various pesticides with different acid-base properties. We selected four pesticides, kinetin, carbendazim, imidacloprid, and isazophos, for validation purposes. Among these, kinetin and carbendazim exhibited a positive charge following hydrolysis, resulting in a marked enhancement in SERS detection efficacy using our method. Conversely, imidacloprid and isazophos did not demonstrate any improvement, as they retained a negative charge post-hydrolysis. Additionally, for negatively charged SERS substrates, the introduction of H^+ can further improve the detection limits. The establishment of this universal and synergistic method enables the straightforward detection of various pesticides using SERS, promising to enhance the practical application of SERS technology in food and agricultural residue detection.

2. Materials and Methods

2.1. Materials

Silver nitrate ($AgNO_3$), sodium hydroxide (NaOH), ammonia solution, sodium chloride (NaCl), sodium carbonate (Na_2CO_3), sodium sulfate (Na_2SO_4), sodium bicarbonate ($NaHCO_3$), methanol (HPLC grade), and anhydrous ethanol were obtained from China National Pharmaceutical Chemical Reagent Co. (Shanghai, China). Rhodamine 6G (R6G), cetylpyridinium chloride monohydrate (CPC), 6-BA, lithium hydroxide (LiOH), sodium citrate ($C_6H_5NaO_7$), and sodium hypophosphite (NaH_2PO_2) were supplied by Aladdin Co., Ltd. (Shanghai, China). Carbendazim and kinetin were provided by Yuanye Biotechnology Co., Ltd. (Shanghai, China). Glass flakes were sourced from Qingdao Xinjingmei Industry and Trade Co. Ultrapure water used in the experiments was produced using a Milli-Q water purification system (Milli-Q; Millipore, USA).

2.2. Preparation of SERS Substrates

The glass substrates loaded with silver nanoparticles (AgNPs@GS) were synthesized by the previous method with a slightly modification[29]. The detailed synthesis procedure was as follows: First, 10 mL of 45 mM silver nitrate ($AgNO_3$) was mixed with 10 mL of a 15 mM cetylpyridinium chloride (CPC) solution, and the mixture was stirred with a magnetic stirrer for 30 min, resulting in a milky-white dispersion. Subsequently, the cleaned glass slides were immersed in this dispersion, and 4 mL of 1 M sodium hydroxide (NaOH) was added. The solution was then placed in a water bath at 35°C under light-excluded synthesis, during which the color of the solution rapidly transitioned from milky white to brown. Ultimately, glass substrates embedded with Ag NPs were successfully synthesized. Prior to this process, the blank glass slides underwent ultrasonic cleaning in ethanol three times, followed by a 24 h immersion in aqua regia. After this treatment, the slides were rinsed with ultrapure water and dried for subsequent use.

2.3. Characterization

The characterization techniques utilized comprised field emission scanning electron microscopy (FESEM, SU8100; Hitachi High-Technologies, Japan) with energy dispersive spectrometry for analyzing the

morphology and size of Ag nanoparticles, UV-visible spectrophotometry for obtaining UV absorption spectra (UV-vis 2450, Shimadzu Corporation, Japan), X-ray diffraction (XRD, Bruker AXS GmbH, Germany) for assessing composition and phase, X-ray photoelectron spectroscopy (XPS, Thermo Fisher Escalab 250Xi, USA) for elemental analysis, optical contact angle (OCA 40, manufactured by Dataphysics Instruments GmbH, Germany) measurement for evaluating hydrophobicity, and nanoparticle size and zeta potential (ZEN3700, Malvern Instruments, UK) analysis for determining particle size distribution and surface charge.

2.4. SERS Detection of 6-BA and Pretreatment and Detection of Bean Sprouts

On the surface of the prepared AgNPs@GS substrate, a dropwise addition method is used to sequentially add a 6-BA standard solution, with each drop volume being 2 μL. After each addition, the next drop is added when the liquid droplet is nearly dry and forms a smaller-sized coffee ring structure, until the cumulative added volume reaches 10 μL. Once the sample is completely dry, the spectral collection is performed on the addition area using a micro-Raman imaging spectrometer, with the specific parameter settings: excitation wavelength of 785 nm, laser power of 20 mW, and a single spectral integration time of 0.25 s.

Purchase fresh, mold-free, bug-free green beans of uniform size from the local market, wash them with deionized water, soak them in deionized water, and germinate for 3 days in the dark at 25±1°C until the desired sprout length (6-8 cm) is reached. The pretreatment of bean sprouts was conducted by integrating national standard methods with the characteristics of the substrate used in this study. The specific procedure is as follows: 10 g of crushed bean sprouts were placed in a centrifuge tube, followed by the addition of 20 mL of methanol. The mixture was subjected to ultrasonic extraction for 15 min and then was centrifuged at 5000 rpm for 10 min to collect the supernatant. This process was repeated twice, and the collected supernatants were combined and subjected to rotary evaporation at 40°C and 60 rpm to remove methanol. Then, redissolve the remaining residue with ammonia solution to a final volume of 5 mL, with a final ammonia concentration of 10 mM. To analyze actual samples, aliquot 10 μL of the redissolved solution and deposit it multiple times on the same area of the AgNPs@GS. Similarly, after drying, was subjected to SERS detection under identical conditions.

2.5. Density Functional Theory (DFT) Calculations

The structures of 6-BA, kinetin, and thiabendazole were optimized using density functional theory (DFT) with the B3LYP functional and the 6-311+G(d) basis set, as implemented in Gaussian 16W software. Normal mode analysis was performed using GaussView 6.1. Additionally, the molecular electrostatic potential (MEP) was visualized using the Multiwfn and VMD software packages.

2.6. Statistical Analysis

Raman spectroscopy data were preprocessed with NGSLabSpec software (HORIBA Scientific, Japan) for baseline correction and other data adjustments. Data calculations and graphical representations were conducted using Origin 2024 (OriginLab, USA). All SERS measurements, actual sample detections, and statistical analyses in the text were conducted with at least five independent repetitions ($n \geqslant 5$).

3. Results and Discussion

The synthesis process of AgNPs@GS is illustrated in Figure 1(a). The preparation principle involves self-assembly and in situ reduction to form uniformly distributed silver nanoparticles on a glass substrate. In this process, silver nitrate serves as the source of silver ions, while cetylpyridinium chloride acts as a surfactant to stabilize the nanoparticles. Additionally, sodium hydroxide is employed to increase the pH, facilitating the reduction of silver ions. This approach ultimately achieves high-performance SERS. We initially conducted a preliminary optimization of the synthesis conditions for the substrate by varying the NaOH concentration and the synthesis time (refer to Fig. S1). Scanning electron microscopy (SEM) images were taken to observe the morphology and particle size of silver nanoparticles grown on the glass substrate for growth times of 12 h, 18 h, 24 h, and 30 h, and particle size analysis was conducted using Image J. The results reveal that as the growth time increased, the distribution of silver nanoparticles on the glass substrate transitioned from sparse to dense, with their shape evolving from irregular to more uniform, eventually leading to the emergence of irregular polymer. The results of the contact angle test demonstrate that the substrate possesses excellent hydrophobicity. This hydrophobic property effectively enriches the target substances, thereby significantly enhancing detection sensitivity[30]. Ultimately, we determined that the SERS performance of AgNPs@GS was optimal at a NaOH concentration of 1.0 M and a synthesis duration of 24 hours. The AgNPs@GS exhibited optimal SERS performance when the NaOH concentration was 1 M and the growth time was 24 h. Under optimal conditions (NaOH concentration of 1 M and growth time of 24 h), the diameter of silver nanoparticles on the glass substrate ranged from 40 to 60 nm, displaying a normal distribution (refer to Fig. 1(c)-(d)). This indicates that the glass substrate prepared under these conditions not only has uniform shapes and regular distributions, but also that the gaps between individual silver nanoparticles are approximately 5 nm, which provides strong electromagnetic enhancement of SERS signal.

Furthermore, we characterized the optimized SERS substrate to verify the successful synthesis of the silver nanoparticles. Energy dispersive spectroscopy (EDS) was employed to analyze the distribution of silver elements in the SERS substrate. As shown in Figures 1(e) to (i), the AgNPs@GS primarily consists of oxygen, silicon, and silver elements[31]. Oxygen and silicon mainly originate from the glass itself, while silver is derived from the silver nanoparticles synthesized on the glass surface, confirming the successful synthesis of Ag NPs nanomaterials on the substrate. As illustrated in Figure 1(j), the surface loading of silver nanoparticles significantly enhanced the overall UV absorption of the glass substrate, with a distinct UV absorption peak observed at 303 nm compared to the blank glass substrate[32]. Variations in growth time led to changes in the particle size of silver nanoparticles, resulting in a blue shift of the absorption peak around 303 nm. The X-ray diffraction (XRD) results of the AgNPs@GS (refer to Figure 1(h)) show four distinct peaks at $2\theta = 38.4°$, 44.6°, 64.7°, and 77.7°. These peaks correspond to the crystalline planes (111), (200), (220), and (311) of cubic silver nanoparticles[33, 34](JCPDS#04-0783), indicating successful growth of silver nanoparticles on the glass substrate. In the X-ray photoelectron spectroscopy (XPS) spectrum of the AgNPs@GS, the strongest signal peak corresponds to Ag 3d, representing the chemical environment and oxidation state of silver atoms.

The XPS analysis of AgNPs@GS revealed distinct peaks for Ag $3d_{5/2}$ and Ag $3d_{3/2}$ at binding energies of 368.18 eV and 374.18 eV, respectively (Figure 1l and 1m). The observed spin-orbit splitting of 6.0 eV between these peaks is characteristic of metallic silver (Ag^0) [35] confirming the successful formation of silver nanoparticles in the composite.

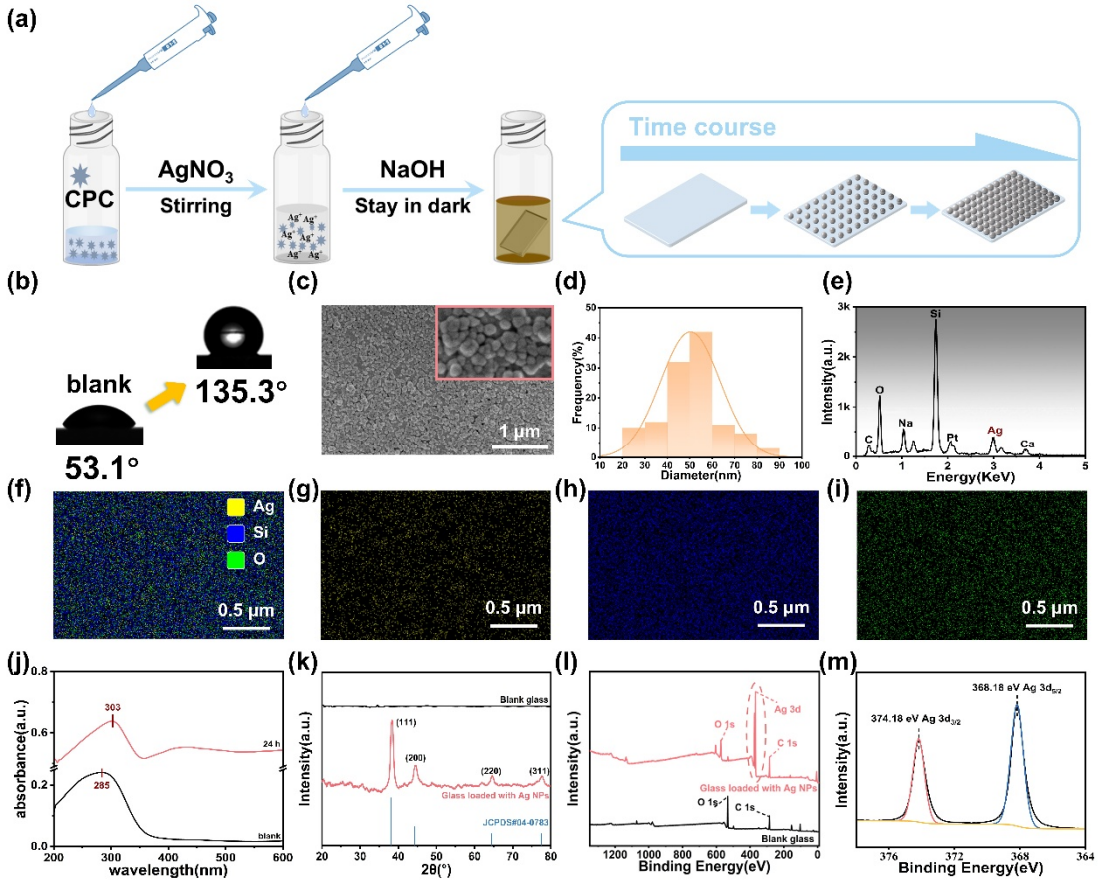

Figure 1. Schematic illustration of the synthesis process of hydrophobic silver nanoparticles substrate (a). Contact angle images of clean glass sheet and AgNPs@GS. (b). The elemental distribution on a specific location of the glass surface during mapping scanning using EDS analysis (c). The corresponding size distributions of Ag NPs the substrates synthesized with 24h (d). The elemental distribution on a specific location of the glass surface during mapping scanning using EDS analysis (c,e): SEM image (c); EDS image (e); The distribution of O, Si, Ag elements (g-i). UV absorption spectra of AgNPs@GS and clean glass at 24 h. (j). XRD results of AgNPs@GS and standard PDF card data of silver nanoparticles (k). High-resolution XPS spectroscopy (l) and AgNPs@GS Ag 3d (m).

Evaluate the SERS enhancement effect, stability, and uniformity of the AgNPs@GS using rhodamine 6G (R6G). Figure 2(a) presents the Raman spectra of glass substrates loaded with AgNPs at varying concentrations of R6G. The SERS spectra, with R6G concentrations ranging from 10^{-11} M to 10^{-6} M, distinctly exhibit characteristic peaks[24] at 613, 774, 928, 1089, 1126, 1183, 1310, 1360, 1510, and 1651 cm^{-1}. Notably, the intensity of the peak at 1510 cm^{-1} increases progressively with rising concentrations of R6G, demonstrating a clear correlation between concentration and signal intensity. This characteristic peak, attributed to the in-plane stretching of the purine ring, was selected for constructing the standard curve due to its strong intensity, minimal shift, and high specificity for 6-BA. The R6G Raman probe molecules achieved an impressive detection limit of 10^{-11} M, indicating that the AgNPs@GS exhibits exceptional sensitivity for direct target detection. The enhancement mechanism can be attributed to the optimized interparticle spacing of the Ag NPs, which significantly amplifies the Raman signal. Under optimal experimental conditions, the Ag

NPs that are grown on the substrate surface exhibit relative uniformity, thereby further enhancing the SERS signal. As shown in Figure 2(b), after being placed in room temperature air for 120 days (without light shielding), the Raman signal of AgNPs@GS still has an enhancement of 74.33%, indicating that the substrate has good stability and possesses certain capabilities for detection in practical complex environments. To further assess the uniformity of the SERS hotspots, we randomly selected 16 measurement points on the surface of the SERS substrate and calculated their respective relative standard deviation (RSD) values. The final standard deviation obtained was 8.45%, indicating excellent uniformity of the SERS substrate in standard pharmaceutical solutions, as demonstrated in Figures 2(c) and (d). Subsequently, we evaluated the stability of the substrate using a 10^{-7} M R6G probe molecule.

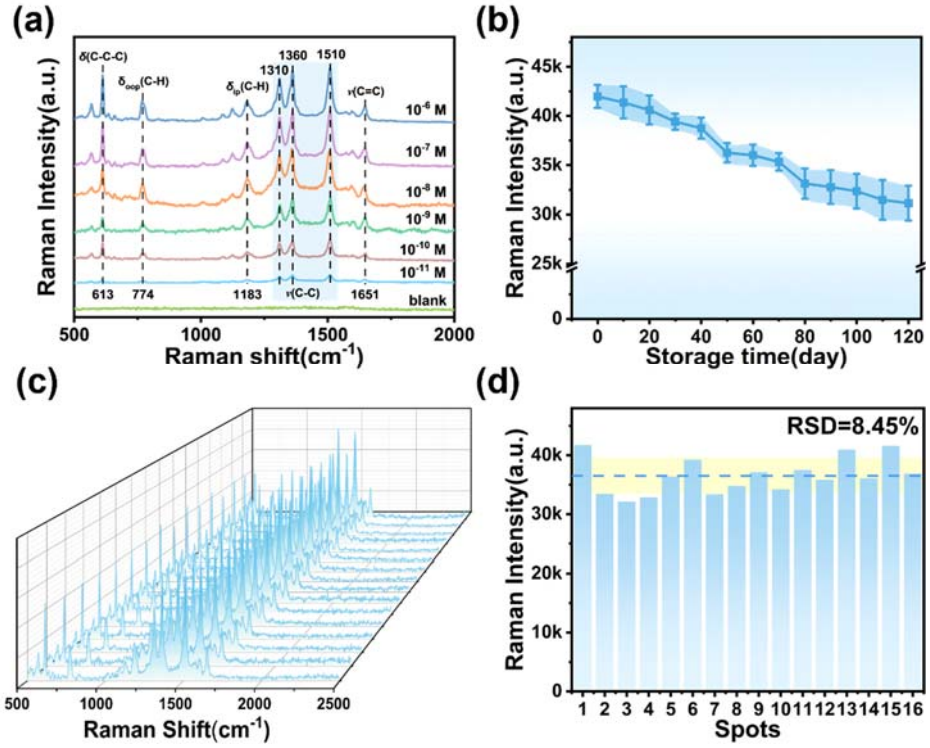

Figure 2. SERS spectrum of different concentrations of R6G solution detected by AgNPs@GS (a). The Raman signal intensity and the corresponding RSD value were measured at 1510 cm^{-1} for 16 randomly selected points during the detection of concentrations of 10^{-7} M R6G solution (b). The R6G solution with concentrations of 10^{-7} M were utilized for detection respectively, and the Raman signal graphs of 16 randomly selected points within the detection regions were captured at random (c). The Raman signal intensity of the AgNPs@GS at 1510 cm^{-1} using a 10^{-7} M R6G solution after being stored at room temperature for various durations (d).

The sample was prepared using the sequential drop-and-dry method outlined in the experimental section, which effectively concentrates the analyte for SERS testing, enabling rapid and efficient detection of pesticide residues. As illustrated in Figure 3(b), the detection limit (LOD) of the AgNPs@GS for the 6-BA standard solution is 0.01 mg/L. According to the requirements of EU Regulation No. 396/2005 (EC), the detection methods used in this study just meet the regulatory standards for pesticide detection. This indicates that the developed SERS substrate has potential applicability in real monitoring scenarios. In the SERS spectrum of the 6-BA pesticide, the Raman intensity at a shift of 1003 cm^{-1} was selected as the dependent variable, while the logarithm of the concentration of the 6-BA standard solution served as the independent variable for the construction of a standard curve. Figure 3(c) presents the linear relationship established through linear

regression analysis within the concentration range of 0.01 to 100 mg/L. The resulting equation for the standard curve is expressed as I_{SERS} = 7829.15 lg (X_C) + 19011.37, with a coefficient of determination (R^2) value of 0.9956, indicating a strong linear correlation with concentration. Notably, even at a concentration as low as 0.01 mg/L, the characteristic peaks of 6-BA at 1003 cm^{-1}, 1215 cm^{-1}, and 1593 cm^{-1} remain distinctly observable. The peak at 1003 cm^{-1} corresponds to the stretching and breathing vibrations of the monosubstituted benzene ring skeleton, the peak at 1215 cm^{-1} is associated with the stretching and breathing vibrations of the benzene ring skeleton, and the peak at 1593 cm^{-1} is attributed to the stretching vibration of the C=N bond.

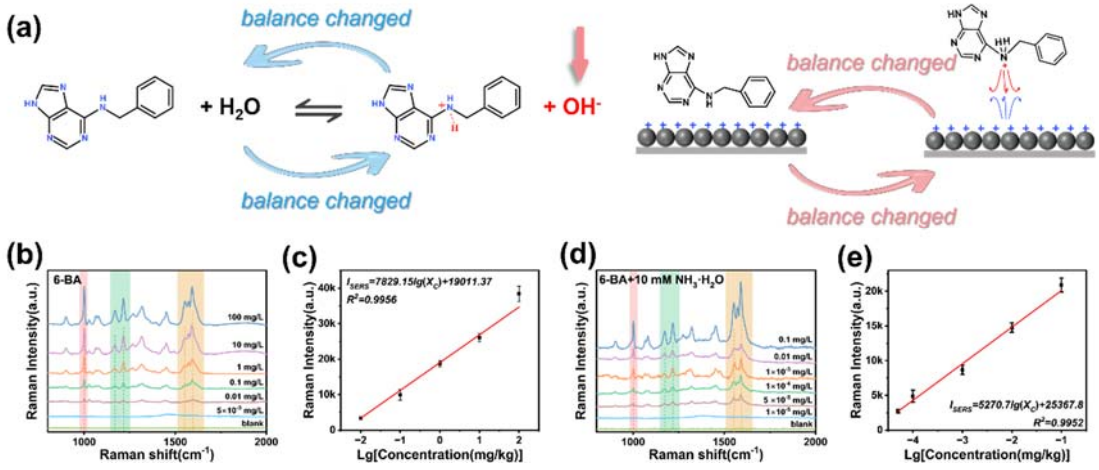

Figure 3. SERS signal enhancement mechanism diagram using 6-BA as an example(a). The Raman spectra of 6-BA solutions at different concentrations were measured by AgNPs@GS (b) and the linear relationship between the logarithm of 6-BA concentration and the intensity of Raman spectra at 1001 cm^{-1} Raman shift(c). The SERS spectra of 6-BA standard solutions with varying concentrations, using ammonia solution as an enhancer(d). Linear relationship between the logarithm of 6-BA solution concentrations and the intensity of the Raman spectra(e).

To further reduce the detection limit of 6-BA to meet actual detection needs, after studying the structure of 6-BA and referencing relevant literature[36], we found that according to Lewis acid theory, the lone pair of electrons on the benzenamine nitrogen atom in the molecule can combine with hydrogen protons in water to undergo hydrolysis, resulting in a positively charged 6-BA molecule. As shown in Appendix Table S1, the silver nanoparticle SERS substrates used in this study are positively charged. We adjusted the concentration of OH^- ions in the solution to modulate the hydrolysis equilibrium, thereby enhancing the electrostatic attraction between the molecule and the SERS substrate, which in turn increases the intensity of the SERS signal. The introduction of OH^- ions may cause changes in the surface charge of the 6-BA molecule, affecting its ability to adsorb onto the silver nanoparticles on the SERS substrate. Alterations in the surface charge of the molecule can enhance the electric field coupling between the molecule and the metal surface, thereby improving the SERS signal[37]. Additionally, OH^- ions may enhance the effectiveness of Raman scattering by altering the molecular conformation or electronic structure of 6-BA. Such structural changes may result in a stronger Raman signal from the molecule when irradiated with laser light (Figure 3(a)).

As illustrated in Figure 3(d), after introducing ammonia water to alter the hydrolysis equilibrium of 6-BA, its detection limit was reduced from 0.01 mg/L to 5×10^{-5} mg/L. Figure 3(e) demonstrates the linear relationship established through linear fitting within the concentration range of 5×10^{-5} to 0.1 mg/L. The

resulting standard curve fitting equation is I_{SERS} = 5270.7 lg(X_C) + 25367.8, with a correlation coefficient (R^2) of 0.9952, indicating a strong linear correlation. These results highlight the significant advantage of this SERS substrate in terms of detection limit, providing a reliable technical foundation for the sensitive detection of 6-BA.

We further evaluated the SERS performance of the substrate by using a bean sprout model with varying concentrations of 6-BA, as detailed in the operational steps shown in Figure 4(a). The SERS spectra of residual 6-BA extracted from the bean sprout samples are presented in Figure 4(b). The results indicate that by applying AgNPs@GS, the detection limit for 6-BA residues in the bean sprouts was achieved as low as 5×10^{-4} mg/kg. This value is substantially lower than the European Union's maximum residue limit (MRL of 0.01 mg/kg for 6-BA in legume vegetables as regulated by EU No. 396/2005), demonstrating not only superior performance compared to previously reported results (refer to Table S2) but also high practical relevance for food safety control. Figure 4(c) illustrates the linear relationship established through linear fitting within the concentration range of 5×10^{-4} to 1 mg/kg. The obtained standard curve fitting equation is I_{SERS} = 2053.81lg (X_C) + 7965.5, with an R^2 value of 0.9932, indicating a strong linear correlation with concentration. The results indicate that AgNPs@GS has significant advantages in detection limits, as it not only enhances the Raman signal intensity through the electromagnetic enhancement effect, but also improves the SERS signal intensity through hydrophobic interactions and the charge interactions between pesticides and surface AgNPs, achieving outstanding detection performance. To assess the reliability of ammonia-assisted AgNPs@GS as a SERS substrate for detecting 6-BA pesticide residues in bean sprouts, we analyzed samples using an established standard curve. Four concentrations within the range of 5×10^{-4} to 1 mg/kg were selected: 1 mg/kg, 0.1 mg/kg, 0.01 mg/kg, and 0.005 mg/kg. The recovery rates obtained were 100.98%, 90.27%, 106.40%, and 91.40%, with corresponding RSD values of 4.59%, 2.19%, 4.24%, and 5.91%. These results indicate that this method is both accurate and reliable for detecting 6-BA pesticide residues in bean sprouts.

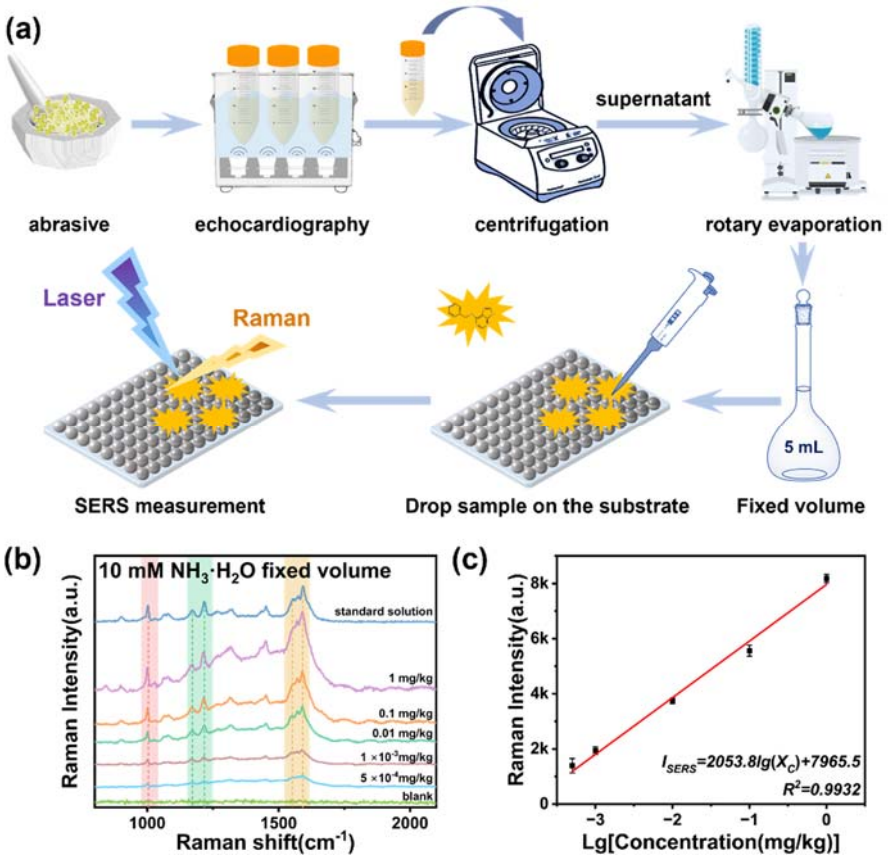

Figure 4. Flowchart illustrating the detection process for actual samples (bean sprouts) (a). The SERS spectra of bean sprouts exhibiting varying residual concentrations, detected using ammonia as a facilitating agent (b). The linear relationship between the logarithm of 6-BA concentration and the intensity of Raman spectrum in the bean sprout model (c).

To investigate the effects of cations and base strength, we thus selected three commercially available, water-soluble bases (NaOH, LiOH, and $NH_3 \cdot H_2O$) and applied them to three Lewis basic pesticides (6-BA, kinetin, and carbendazim) to validate and demonstrate the generality of the method. Figures 5 (a)-(c) illustrate the molecular structures and charge distributions of each compound, with colors representing variations in charge density. The molecular electrostatic potential maps reveal the electronic characteristics within the molecules by depicting their charge distributions[38]. The results indicate that these molecules may undergo protonation in aqueous solution, similar to 6-BA. As illustrated in Figure 5, our findings revealed that after adding varying concentrations of NaOH, LiOH, and ammonia water, the SERS signals of these three pesticide molecules significantly increased, even when maintaining the same concentration of the standard solution. This notable enhancement in signal intensity suggests that the proposed method is not only effective but also exhibits a certain degree of universality across different Lewis basic pesticides. Moreover, similarly, applying this method to Lewis acidic pesticides (Figure S3) reveals that the introduction of ammonia can further promote the hydrolysis of these pesticides, increasing the number of negatively charged pesticide molecules on the surface, thereby enhancing the interaction with the substrate and boosting the SERS detection signal. In summary, based on the conclusions of this study and Lewis acid-base theory, the interaction between the target analyte and the SERS substrate can be effectively enhanced by adding an acid or a base according to the surface charge of the SERS substrate and the hydrolysis condition of the detected molecules, which can effectively lower the detection limit to meet practical detection needs.

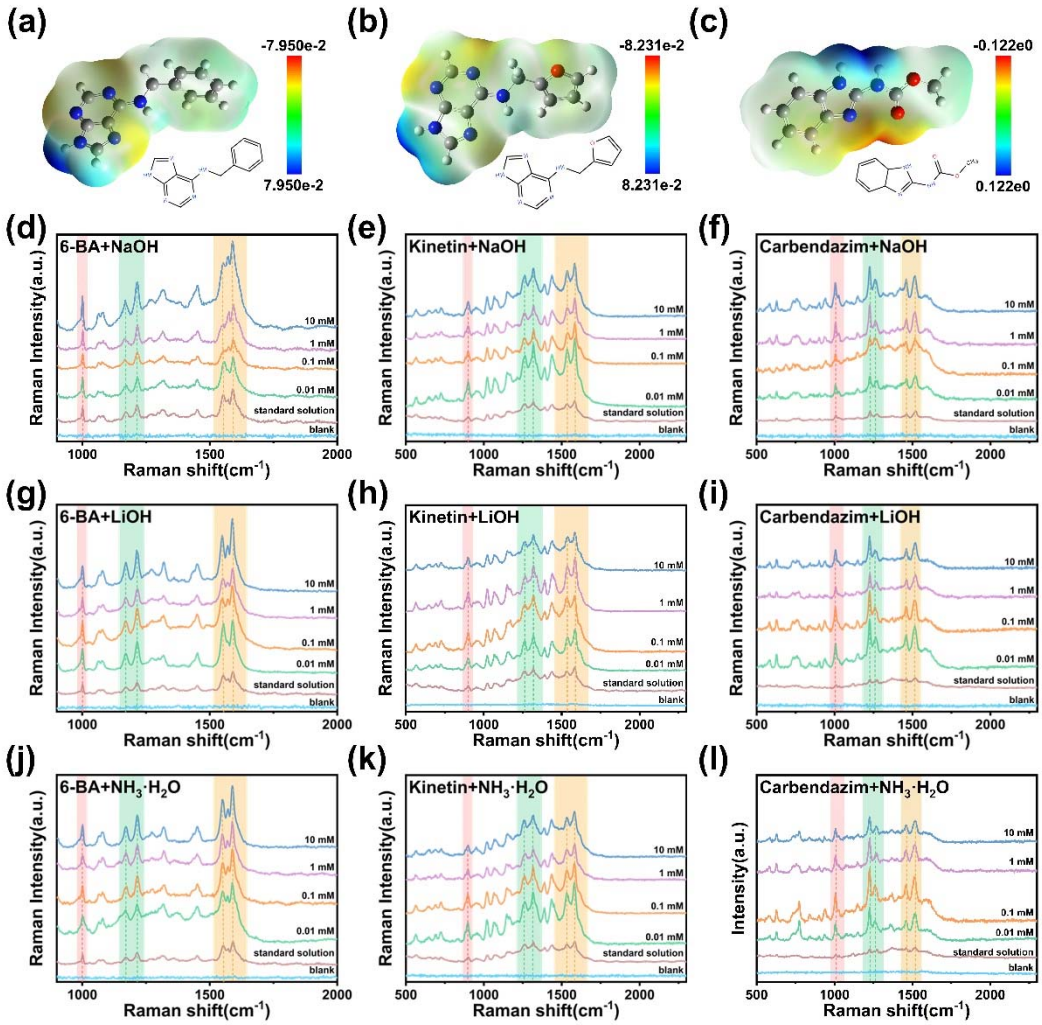

Figure 5. Structural formula and surface potential distribution of 6-BA, kinetin and carbendazim(a-c).The SERS spectra of 6-BA, kinetin and carbendazim at a concentration of 1 mg/L obtained using NaOH solutions of varying concentrations(d-f);The SERS spectra of 6-BA,kinetin and carbendazim at a concentration of 1 mg/L obtained using LiOH solutions of varying concentrations(g-i).The SERS spectra of 6-BA, kinetin and carbendazim at a concentration of 1 mg/L obtained using ammonia solutions of varying concentrations (j-l).

4. Conclusions

Overall, we synthesized a hydrophobic SERS substrate with exceptional stability and uniformity. This substrate exhibited outstanding SERS performance, achieving a detection limit of 10^{-11} M for R6G molecules, and demonstrated remarkable stability. Utilizing Lewis acid-base theory, we successfully facilitated the hydrolysis reaction of basic pesticides, resulting in a two-order-of-magnitude reduction in the detection limit for 6-BA. In practical tests using a bean sprout model, we detected residual concentrations of 6-BA as low as 5×10^{-4} mg/kg. This method is not only applicable to the detection of 6-BA but has also been extended to other similar basic pesticides, revealing analogous phenomena. In conclusion, our research demonstrates the applicability of Lewis acid-base theory in optimizing pesticide detection methods. By strategically adding acids or bases based on the surface charge of the SERS substrate, we can enhance the electrostatic interactions between the target substance and the substrate. This effectively reduces the detection limit, making it more applicable for practical pesticide detection and paving the way for further exploration of SERS applications in environmental monitoring and agricultural safety.

Declaration of Interest Statement

The authors declare no competing financial interests or personal relationships that could have appeared to influence the work reported in this paper.

Acknowledgement

This project was financially supported by the Natural Science Foundation of China (32261133623, 22073014), the National Key R&D Program of China (2022YFF1100803), the Fundamental Research Funds for the Central Universities (Grant nos. 2572023CT12) and Postgraduate Research & Practice Innovation Program of Jiangsu Province (KYCX24_2625).

Reference

[1] H.P. Li, E. Dumont, R. Slipets, et al., Democratizing robust SERS nano-sensors for food safety diagnostics, Chem Eng J. 470 (2023) https://doi.org/10.1016/j.cej.2023.144023.

[2] B.X. Hu, H.B. Pu, D.W. Sun, Multifunctional cellulose based substrates for SERS smart sensing: Principles, applications and emerging trends for food safety detection, Trends Food Sci Tech. 110 (2021) 304-320. https://doi.org/10.1016/j.tifs.2021.02.005.

[3] K. Chang, Y.J. Zhao, Z.X. Xu, et al., Advances in metal-organic framework-plasmonic metal composites based SERS platforms: Engineering strategies in chemical sensing, practical applications and future perspectives in food safety, Chem Eng J. 459 (2023) https://doi.org/10.1016/j.cej.2023.141539.

[4] Q.Q. Quan, Z.W. Liu, Z.D. Li, et al., Authenticating Emergent Adulterant 6-Benzylaminopurine in Bean Sprouts: Virtual Hapten Similarity Enhanced Immunoassay, Journal of Agricultural and Food Chemistry. 71 (2023) 8203-8210. https://doi.org/10.1021/acs.jafc.3c01696.

[5] X. Pang, J. Qiu, Z.Y. Zhang, et al., Wide-Scope Multi-residue analysis of pesticides in beef by gas chromatography coupled with quadrupole Orbitrap mass spectrometry, Food Chemistry. 407 (2023) 135171. https://doi.org/10.1016/j.foodchem.2022.135171.

[6] H. Kim, E.J. Baek, Y.K. Kim, et al., Development of a method for analysis and risk assessment of residual pesticides in ginseng using liquid and gas chromatography-tandem mass spectrometry, Food Chemistry. 427 (2023) 136675. https://doi.org/10.1016/j.foodchem.2023.136675.

[7] W.Y.Z. Guo, Y.X. Fu, S.Y. Liu, et al., Multienzyme-Targeted Fluorescent Probe as a Biosensing Platform for Broad Detection of Pesticide Residues, Analytical Chemistry. 93 (2021) 7079-7085. https://doi.org/10.1021/acs.analchem.1c00553.

[8] S.Y. Wang, Q.X. Hao, Y.N. Zhao, Y.S. Chen, Two-Dimensional Printed AgNPs@Paper Swab for SERS Screening of Pesticide Residues on Apples and Pears, Journal of Agricultural and Food Chemistry. 71 (2023) 4982-4989. https://doi.org/10.1021/acs.jafc.3c00134.

[9] D.C. Yang, B. Youden, A. Carrier, et al., Nanomaterials for surface-enhanced Raman spectroscopy-based metal detection: a review, Environ Chem Lett. 22 (2024) 2425-2465. https://doi.org/10.1007/s10311-024-01758-8.

[10] C.C. Huang, Z.H. Hsu, Y.S. Lai, Raman spectroscopy for virus detection and the implementation of unorthodox food safety, Trends Food Sci Tech. 116 (2021) 525-532. https://doi.org/10.1016/j.tifs.2021.08.008.

[11] S.Y. Wang, Y.N. Zhao, X. Wei, Y.S. Chen, Facile SERS screening of melamine in bovine milk with 2D printed AgNPs/glass fabric filter paper as the flexible substrate, Food Science and Human Wellness. 13 (2024) 2595-2600. https://doi.org/10.26599/fshw.2022.9250208.

[12] L. Fabris, SERS on semiconductor substrates receives an electromagnetic boost, Chem-Us. 9 (2023) 1349-1352. https://doi.org/10.1016/j.chempr.2023.05.021.

[13] H.Y. Yang, H.R. Mo, J.Z. Zhang, et al., Observation of single-molecule Raman spectroscopy enabled by synergic electromagnetic and chemical enhancement, Photonix. 5 (2024) https://doi.org/10.1186/s43074-024-00119-6.

[14] X.Y. Liu, Z.W. Ye, Q. Xiang, et al., Boosting electromagnetic enhancement for detection of non-adsorbing analytes on semiconductor SERS substrates, Chem-Us. 9 (2023) 1464-1476. https://doi.org/10.1016/j.chempr.2023.01.017.

[15] B. Yang, G. Chen, A. Ghafoor, et al., Chemical Enhancement and Quenching in Single-Molecule Tip-Enhanced Raman Spectroscopy, Angew Chem Int Edit. 62 (2023) https://doi.org/10.1002/anie.202218799.

[16] S. Cong, X.H. Liu, Y.X. Jiang, et al., Surface Enhanced Raman Scattering Revealed by Interfacial Charge-Transfer Transitions, Innovation-Amsterdam. 1 (2020) https://doi.org/10.1016/j.xinn.2020.100051.

[17] J. Cheng, Y. Shen, Y.L. Gu, et al., Metal-polyphenol Multistage Competitive Coordination System for Colorimetric Monitoring Meat Freshness, Adv. Mater. 37 (2025) https://doi.org/10.1002/adma.202503246.

[18] H.Y. Gu, L.J. Hu, Y.N. Dong, et al., Evolving trends in fluorescence spectroscopy techniques for food quality and safety: A review, J Food Compos Anal. 131 (2024) https://doi.org/10.1016/j.jfca.2024.106212.

[19] B.Z. Li, S.J. Liu, L.J. Huang, et al., Nanohybrid SERS substrates intended for food supply chain safety, Coordin Chem Rev. 494 (2023) https://doi.org/10.1016/j.ccr.2023.215349.

[20] Q. Yang, D.W. Sun, H.B. Pu, Porous materials nanohybridized with metal nanoparticles as substrates for enhancing SERS detection in food safety applications, Trends Food Sci Tech. 141 (2023) https://doi.org/10.1016/j.tifs.2023.104202.

[21] J. Cheng, S.Q. Zhuang, Z.W. Luo, et al., Simple and rapid capillarity-assisted ultra-trace detection of thiram on apple surface with a silver nanoparticles/filter paper SERS substrate, Journal of Hazardous Materials. 485 (2025) 136945. https://doi.org/10.1016/j.jhazmat.2024.136945.

[22] W.W. Cheng, X.Z. Tang, Y. Zhang, et al., Applications of metal-organic framework (MOF)-based sensors for food safety: Enhancing mechanisms and recent advances, Trends Food Sci Tech. 112 (2021) 268-282. https://doi.org/10.1016/j.tifs.2021.04.004.

[23] C.Y. Zhang, L.J. Huang, H.B. Pu, D.W. Sun, Magnetic surface-enhanced Raman scattering (MagSERS) biosensors for microbial food safety: Fundamentals and applications, Trends Food Sci Tech. 113 (2021) 366-381. https://doi.org/10.1016/j.tifs.2021.05.007.

[24] S.Q. Zhuang, J. Cheng, S.T. Chen, et al., Lotus leaf-inspired biomimetic SERS substrate for detection of thiram on apple, Food Bioscience. 58 (2024) 103818. https://doi.org/10.1016/j.fbio.2024.103818.

[25] X.Y. Liu, W. Deng, Y.Z. Yang, et al., Superhydrophobic nanocellulose-based self-assembled flexible SERS substrates for pesticide detection, International Journal of Biological Macromolecules. 282 (2024) 137171. https://doi.org/10.1016/j.ijbiomac.2024.137171.

[26] Y.Y. Gao, Y.Q. Wan, L. Liu, et al., Highly sensitive sensing and quantitative detection of sulfate ion with a SERS chip-based on boric acid's Lewis effect, Analytical Sciences. 38 (2022) 1385-1394. https://doi.org/10.1007/s44211-022-00169-5.

[27] X.J. Chen, X.X. Huang, S.L. Chen, et al., Alkali hydrolysis and Lewis acids assisted enhancement based highly sensitive and quantitative detection of malathion in tea using SERS and multivariate analysis, Sensors and Actuators B-Chemical. 359 (2022) 131584. https://doi.org/10.1016/j.snb.2022.131584.

[28] J. Shang, F.N. Niu, Z.W. Cai, et al., Inhibition-type SERS strategy based on silver nanowires@ZrO2 composite substrate: Achieving high-sensitivity and specific detection of methyl parathion, Microchemical Journal. 215 (2025) 114460. https://doi.org/10.1016/j.microc.2025.114460.

[29] Q.Q. Peng, N. Wang, Y. Zhu, et al., Hydrophobic AgNPs: one-step synthesis in aqueous solution and their greatly enhanced performance for SERS detection, J Mater Chem C. 7 (2019) 10465-10470. https://doi.org/10.1039/c9tc03143j.

[30] S. Shin, J. Lee, S. Lee, et al., A Droplet-Based High-Throughput SERS Platform on a Droplet-Guiding-Track-Engraved Superhydrophobic Substrate, Small. 13 (2017) https://doi.org/10.1002/smll.201602865.

[31] K. Haruna, T.A. Saleh, Dopamine functionalized graphene oxide (DGO) as a corrosion inhibitor against X60 carbon steel corrosion in a simulated acidizing environment; An electrochemical, weight loss, SERS, and computational study, Surf Interfaces. 44 (2024) https://doi.org/10.1016/j.surfin.2023.103688.

[32] J.L. Cholula-Díaz, D. Lomelí-Marroquín, B. Pramanick, et al., Synthesis of colloidal silver nanoparticle clusters and their application in ascorbic acid detection by SERS, Colloid Surface B. 163 (2018) 329-335. https://doi.org/10.1016/j.colsurfb.2017.12.051.

[33] M. Shariat, Plasma jet printing of silver nanoparticles on polyester fabric as a surface-enhanced Raman scattering substrate, Optik. 277 (2023) https://doi.org/10.1016/j.ijleo.2023.170698.

[34] S.K. Vemuri, S. Mukhopadhyay, A. Ray, I. Mukhopadhyay, 3D SERS substrate using silver nanoparticles decorated ZnO nanorods on silicon micropyramids hybrid heterostructure, Appl Surf Sci. 675 (2024) https://doi.org/10.1016/j.apsusc.2024.160993.

[35] X.Y. Han, Y. Wang, T.Y. Wang, et al., Ultra-sensitive mercury detection from surface wrapping of carbon dots reduced and decorated silver nanoparticles on SERS fiber probes, J Alloy Compd. 976 (2024) https://doi.org/10.1016/j.jallcom.2023.173085.

[36] I. Pilarova, P. Lubal, L. Trnkova, Potentiometric and Voltammetric Study of 6-Benzylaminopurine and Its Derivatives, Electroanalysis. 24 (2012) 349-356. https://doi.org/10.1002/elan.201100491.

[37] D.J. Kim, S.G. Park, D.H. Kim, S.H. Kim, SERS-Active-Charged Microgels for Size- and Charge-Selective Molecular Analysis of Complex Biological Samples (vol 14, 1802520, 2018), Small. 14 (2018) https://doi.org/10.1002/smll.201804655.

[38] N. Singh, A. Fatima, M. Singh, et al., Exploration of experimental, theoretical, Hirshfeld surface, molecular docking and electronic excitation studies of Menadione: A potent anti-cancer agent, J Mol Liq. 351 (2022) https://doi.org/10.1016/j.molliq.2022.118670.